

with the calculations. One of us (MMS) wishes to acknowledge useful conversations with Professor D. Koltun and Professor L. Kisslinger.

*Research supported in part by the National Science Foundation.

†Research supported in part by the U. S. Atomic Energy Commission.

¹E. H. Auerbach, D. M. Fleming, and M. M. Sternheim, *Phys. Rev.* **162**, 1683 (1967), and **171**, 1781 (1968).

²L. S. Kisslinger, *Phys. Rev.* **98**, 761 (1955).

³F. Binon, P. Duteil, J. P. Garron, J. Gorres, L. Hugun, J. P. Peigneux, C. Schmit, M. Spighel, and J. P. Stroot, *Nucl. Phys.* **B17**, 168 (1970).

⁴D. Koltun, *Advan. Nucl. Phys.* **3**, 71 (1969).

⁵D. T. Chivers, E. M. Rimmer, B. W. Allardyce, R. C. Whitcomb, J. J. Domingo, and N. W. Tanner, *Nucl. Phys.* **A126**, 129 (1969); P. W. Hewson, *Nucl. Phys.* **A133**, 659 (1969).

⁶K. M. Watson, *Phys. Rev.* **118**, 886 (1960), and earlier references given here.

⁷E. H. Auerbach and M. M. Sternheim, BNL Report No. 12696 (1968).

⁸L. Moyer and D. S. Koltun, *Phys. Rev.* **182**, 999 (1969).

⁹M. L. Goldberger and K. M. Watson, *Collision Theory*, (Wiley, New York, 1964), p. 688.

¹⁰D. G. Ravenhall, *Rev. Mod. Phys.* **30**, 430 (1958).

¹¹Using free parameters without the Fermi averaging yields curves similar to those in Fig. 1 and 2 but with a slightly poorer fit to the data at all energies.

¹²Variation of b_0 did not significantly improve agreement with the data.

Anomalies in the Cross Sections of (d, n) Reactions Leading to Isobaric Analog States*

S. A. A. Zaidi, C. L. Hollas, J. L. Horton, and P. J. Riley
The University of Texas at Austin, Austin, Texas 78712

and

J. L. C. Ford, Jr., and C. M. Jones
Oak Ridge National Laboratory, Oak Ridge, Tennessee 37830
(Received 17 August 1970)

The (d, n) reactions on the nuclei ^{92}Mo , ^{94}Mo , ^{96}Mo , and ^{96}Zr leading to the isobaric analog states in the residual nuclei have been studied. The observed (d, n)-reaction cross sections show strong deviations from the distorted-wave Born-approximation calculations based upon the known neutron spectroscopic factors of the corresponding parent analog states.

In this communication we present evidence that the (d, n) reactions on several target nuclei in the $N=50$ region leading to the isobaric analog states of the target-plus-neutron system display anomalous behavior. The anomalies consist of large deviations of the observed (d, n)-reaction cross sections from the values predicted by distorted-wave Born-approximation (DWBA) calculations. We find that the (d, n) cross sections for the reaction leading to $d_{5/2}$ and $d_{3/2}$ isobaric analog states are strongly enhanced, whereas those leading to $s_{1/2}$ isobaric analog states tend to be smaller than the DWBA values. For almost all of the nuclei studied, the isobaric analog of the ground state of the target-plus-neutron system is populated far more strongly than any other isobaric state. Recently, McGrath et al.¹ have reported the measurement of ($^3\text{He}, d$) cross sections on $^{90,92,94}\text{Zr}$ and $^{92,94,96,98}\text{Mo}$ targets to unbound isobaric analog states. All expected tran-

sitions are observed in their work except those to $3s_{1/2}$ analog states which are inhibited. Preliminary attempts to understand this anomaly in terms of the distorted-wave Born approximation have been reported to be unsuccessful.

The data in the present work were obtained during a systematic study of the (d, n) reaction as a tool for obtaining information on the single-proton character of states in the $N \cong 50$ region.² The experiments were performed using the Oak Ridge National Laboratory tandem Van de Graaff accelerator in conjunction with the pulsed and bunched-ion source. The experimental equipment and procedures have been described elsewhere.³ The deuteron-beam energy was 12 MeV, and the neutron flight path from the target to the detector was 12 m. Rolled foils of ^{92}Mo ($910 \mu\text{g}/\text{cm}^2$), ^{94}Mo ($1 \text{ mg}/\text{cm}^2$), ^{96}Mo ($960 \mu\text{g}/\text{cm}^2$), and ^{96}Zr ($450 \mu\text{g}/\text{cm}^2$) were used as targets. Figure 1 shows four (d, n) neutron time-of-flight spectra

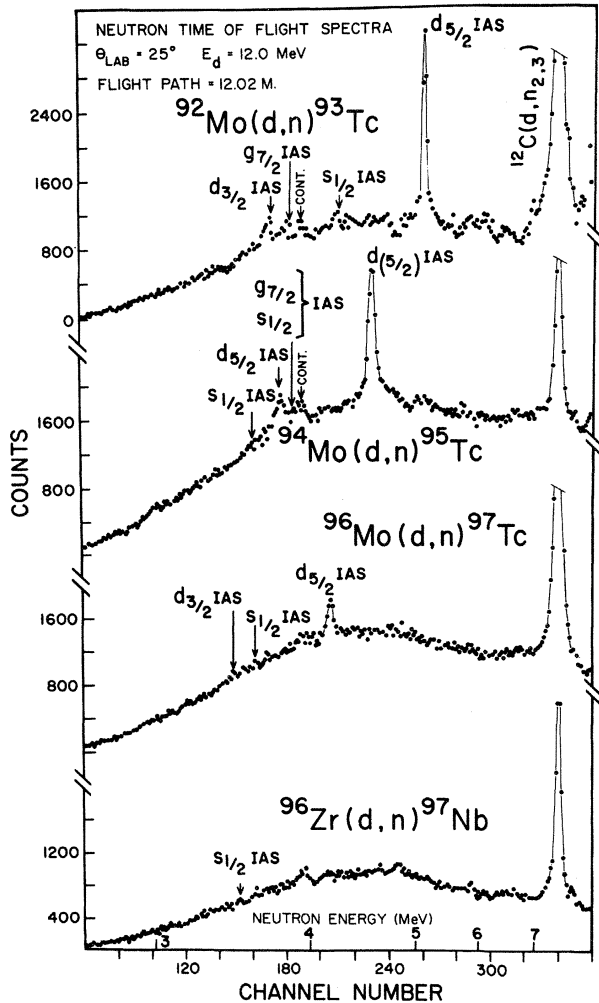


FIG. 1. Neutron time-of-flight spectra obtained by bombarding ^{92}Mo , ^{94}Mo , ^{96}Mo , and ^{96}Zr targets with 12.0-MeV deuterons. For simplicity, parts of the spectra showing neutron groups corresponding to the population of low-lying states of the residual nuclei have been deleted.

obtained from the respective targets ^{92}Mo , ^{94}Mo , ^{96}Mo , and ^{96}Zr at a laboratory angle of 25° . For simplicity, parts of the neutron spectra showing neutron groups corresponding to the population of the low-lying states in ^{93}Tc , ^{95}Tc , ^{97}Tc , and ^{97}Nb have been deleted. The neutron group on the extreme right in each spectrum is from the reaction $^{12}\text{C}(d, n_{2,3})^{13}\text{N}$, resulting from carbon contamination in the targets. The neutron groups corresponding to $d_{5/2}$ transitions to states in ^{93}Tc , ^{95}Tc , and ^{97}Tc , which are analogs of the ground states of the target plus neutron, are indicated on the spectra. Neutron groups leading to the $d_{3/2}$ isobaric analog states in ^{93}Tc and to the $l=2$ excited state with tentative spin $\frac{5}{2}$ in ^{95}Tc

are also seen. The arrows show the expected positions of neutron groups corresponding to the population of those low-lying analog states whose parent states have large spectroscopic factors. Neutrons leading to the $s_{1/2}$ analog state in ^{93}Tc are observed weakly. Identification of the above states has been made on the basis of their expected flight times, and all of the above states have been identified at two or more angles of observation. No other transitions leading to analog states can be identified in the spectra. It should be understood when examining Fig. 1 that the neutron-detection efficiency decreases with decreasing neutron energy. Between 5 and 3.5 MeV, the neutron-detection efficiency decreases by nearly a factor of 2. The neutron bias energy was 2.7 MeV.

In ^{95}Tc , the low-lying $g_{7/2}$ and $s_{1/2}$ analog states are not expected to be resolved; the peaks due to both these states occur very close to a contaminant line in the spectra, but both clearly have very small cross sections. In the case of $^{96}\text{Zr}(d, n)^{97}\text{Nb}^A$, the (d, n) reaction to the $s_{1/2}$ state is so weak that it is not observed, even though in this case it is the analog of the target-plus-neutron ground state. Additional data taken have been at laboratory angles of 15.5° , 20° , and angles greater than 25° . At all the angles the data are consistent with the results shown at 25° . In summary, (a) the $d_{5/2}$ ground-state analogs are populated much more strongly than the analog of any of the excited states of the present analog nuclei, and (b) the $s_{1/2}$ and $g_{7/2}$ analog states are populated very weakly. We have also observed this behavior in the reaction $^{90}\text{Zr}(d, n)$.

The results are presented in Table I. The first column gives the center-of-mass energy of the proton emitted in the decay of the analog state; that is, the center-of-mass energy of the analog resonance observed in proton elastic scattering. The next three columns list the binding energies, spins, and neutron spectroscopic factors S_n of the parent analog states.^{4,6-8} Most of the neutron spectroscopic factors have been taken as indicated in the table from the (d, p) work of Moorhead and Moyer.⁴ In the fifth column is tabulated $2T_0 + 1$ times the proton spectroscopic factors of the corresponding isobaric analog states, S_p , deduced in the present work. Columns 6 and 7 give the observed center-of-mass differential cross sections for the neutron groups leading to the respective analog states at laboratory angles of 15.5° and 25° . Where a particular state could not be identified in the spectra, an approximate

Table I. A comparison of measured (d,n) -reaction cross sections leading to isobaric analog states with DWBA calculations. The calculations were performed assuming the form factor of the transferred proton to be the same as that of the neutron in the parent analog state. The anomalies consist in the large measured (d,n) cross sections for the $d_{5/2}$ and $d_{3/2}$ states shown in columns 6 and 7 as compared with the DWBA calculations given in columns 8 and 9.

| Target Nucleus | C.M. Energy of Decay Proton (1) | Parent Analog State | | | $(2T_0+1)S_p$ (5) | $\left(\frac{d\sigma}{d\Omega}\right)_{\theta_n=15.5^\circ}$ $\mu\text{b/sr}$ (6) | From the (d,n) Reaction $\theta_n=25^\circ$ (7) | $\left(\frac{d\sigma}{d\Omega}\right)_{\text{DWBA}}$ $\mu\text{b/sr}$ | | Γ_{tot} (keV) Analog State (10) |
|------------------|---------------------------------|---------------------|---------------|-----------|-------------------|---|---|---|----------------|---|
| | | B_n (MeV) (2) | J^π (3) | S_n (4) | | | | 15° (8) | 25° (9) | |
| ^{92}Mo | 4.32(c) | 8.06 | $5/2^+$ (a) | 0.84(a) | 2.88 | 2000 ± 200 | 1200 ± 200 | 480 | 410 | ~ 1 |
| | 5.25(c) | 7.13 | $1/2^+$ (a) | 0.64(a) | .28 | 130 ± 30 | 100 ± 30 | 290 | 85 | 41 (c) |
| | 5.68(a) | 6.70 | $7/2^+$ (a) | 0.26(a) | 1.62 | Contaminant | ≤ 100 | 4 | 9 | |
| | 5.83(c) | 6.55 | $3/2^+$ (a) | 0.50(a) | | 500 ± 50 | 300 ± 50 | 130 | 116 | 27 (c) |
| ^{94}Mo | 4.91(c) | 7.38 | $5/2^+$ (a) | 0.59(a) | 4.1 | 2000 ± 150 | 1300 ± 150 | 230 | 202 | 18 (c) |
| | 5.67(a) | 6.62 | $7/2^+$ (a) | 0.18(a) | | ≤ 50 | ≤ 100 | 110 | 19 | |
| | 5.68(c) | 6.61 | $1/2^+$ (a) | 0.37(a) | | | | | | |
| | 5.74(c) | 6.55 | $(5/2^+)$ (a) | 0.17(a) | | Contaminant | 360 ± 50 | 56 | 49 | 45 (c) |
| ^{96}Mo | 5.33(c) | 6.82 | $5/2^+$ (c) | 0.42(e) | 1.56 | 500 ± 50 | 300 ± 50 | 112 | 104 | 33 (c) |
| | 6.00(c) | 6.15 | $1/2^+$ (c) | 0.68(c) | | ≤ 40 | ≤ 40 | 120 | 20 | 68 (c) |
| | 6.09(c) | 6.06 | $3/2^+$ (c) | 0.27(c) | | ≤ 40 | ≤ 40 | | | 33 (c) |
| ^{96}Zr | 6.07(d) | 5.58 | $1/2^+$ (d) | 0.98(b) | | ≤ 40 | ≤ 60 | 200 | 40 | 90 (d) |

^aRef. 4.^bRef. 6.^cRef. 7.^dRef. 9.^eRef. 5.

upper limit to the cross section is given. Columns 8 and 9 give the corresponding theoretical DWBA cross sections. The theoretical cross sections have already been divided by the factor $2T_0+1$, and then multiplied by the neutron spectroscopic factor given in column 4. The last column gives the total widths in keV of the isobaric analog resonances, obtained from proton elastic-scattering data.

Ideally, one expects the neutron spectroscopic factor of a state to be related to the proton spectroscopic factor of its isobaric analog state by the equation

$$S_p = (2T_0 + 1)^{-1} S_n.$$

Comparison of the corresponding entries in columns 4 and 5 shows the anomalous behavior of the proton spectroscopic factors mentioned above. Following the above relations one would again expect the entries in columns 8 and 9 to agree with the corresponding ones in 6 and 7.

The DWBA calculations were performed assuming the form factor of the transferred proton to be the same as that of the neutron in the corresponding parent analog state. The neutron and deuteron optical-model parameters chosen gave good DWBA fits to the (d,n) data for the low-lying

states in ^{93}Tc . The deuteron optical-model parameters in the usual notation are $V_0 = 88$ MeV, $W_d = 14.0$ MeV, $V_{s0} = 6.0$ MeV, $r_{or} = 1.25$ F, $r_{ol} = 1.41$ F, $r_{s0} = 1.20$ F, $r_c = 1.30$ F, $a_r = 0.727$ F, $a_l = 0.694$ F, and $a_{s0} = 0.687$ F. The neutron optical-model parameters used were $V_0 = 46$ MeV, $W_d = 9.3$ MeV, $V_{s0} = 6.5$ MeV, $r_{or} = 1.26$ F, $r_{ol} = 1.23$ F, $r_{s0} = 1.20$ F, $r_c = 1.21$ F, $a_r = 0.66$ F, $a_l = 0.48$ F, and $a_{s0} = 0.50$ F. The fits obtained for the isobaric analog states are shown in Fig. 2. As a check on the DWBA calculations we analyzed the (d,n) -reaction cross sections to the low-lying states in ^{93}Tc and obtained proton spectroscopic factors. Our spectroscopic factors are somewhat smaller than those reported by Picard and Bassani⁹ using the $(^3\text{He},d)$ reaction; however, these authors employed arbitrary normalization to satisfy the sum rule. Thus the DWBA calculations employing the above parameters tend, if anything, to underestimate the spectroscopic factors slightly.

We conclude that there is evidence that the yield of these (d,n) reactions leading to isobaric analog states depends strongly on the l value of the transferred proton, and possibly on the energy of the final state populated. The analog states subsequently decay either through the

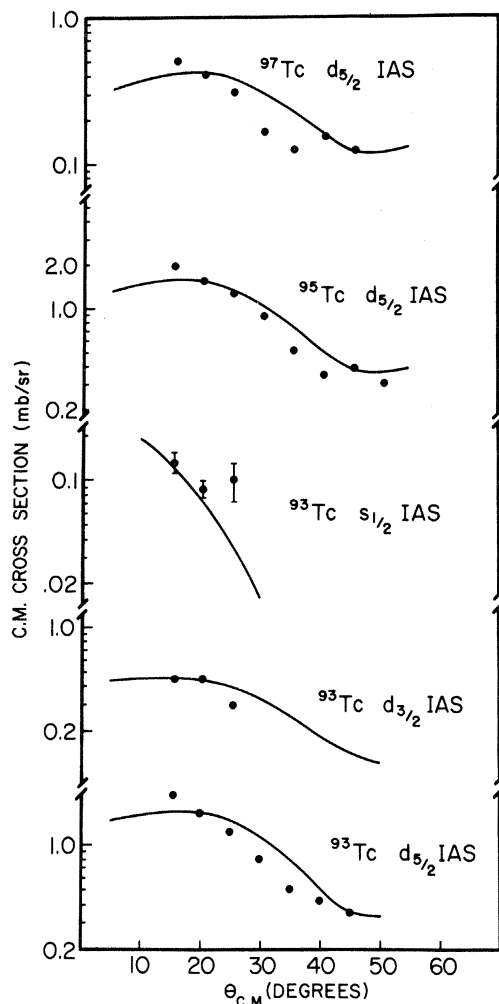


FIG. 2. Angular distributions and DWBA calculations for five strong (d,n) reactions leading to the isobaric analog states in the residual nuclei.

emission of a proton or of a neutron. These proton-unstable final states have also been studied by bombarding the corresponding target nuclei with protons of appropriate energy.⁷⁻⁹ The total widths of the analog resonances observed range between a few keV for the $d_{5/2}$ ground-state analogs of ^{93}Mo and ^{91}Zr to 90 keV for the $s_{1/2}$ ground-state analog of ^{97}Zr . The lifetime τ of a state with a width Γ of 100 keV is approximately 6×10^{-21} sec; a neutron emitted in the (d,n) reaction with an energy of 4 MeV would travel 1.75×10^{-11} cm, a distance of more than 15 nuclear diameters, during this time. Thus one is tempted to believe that it would be a good approximation to treat the isobaric analog state as a bound state obtained by applying the isospin-lowering operator $T^{(-)}$ upon the parent analog state.

The DWBA calculations displayed in Fig. 2 and the spectroscopic factors S_p given in the fifth column of Table I are based upon this approximation. The calculations fail to predict the anomalous behavior displayed by the observed cross sections. We believe that the naive picture of the reaction process, which is based upon the approximation that the final state of the (d,n) reaction is obtained by applying the isospin-lowering operator $T^{(-)}$ to the parent analog state, is inadequate.

The present work corroborates the ($^3\text{Hd}, d$) measurements of McGrath et al.¹ to the extent that the (d,n) -reaction cross sections for populating the analog states also show strong deviations from the predictions of a DWBA calculation which treats the analog resonances as bound states. The ($^3\text{He}, d$) data indicate a strong inhibition of $3s_{1/2}$ analog states. In the (d,n) work the $3s_{1/2}$ analog states are also somewhat inhibited, but the most pronounced effect is the strong enhancement of $2d_{5/2}$ and $2d_{3/2}$ analog states. At present it is not clear to us whether both anomalies have a common origin in the fact that the reactions studied lead to unbound final states. It is, however, conceivable that the proton form factor of the analog resonance deviates appreciably from the neutron form factor of the parent analog state and that this deviation affects the two reactions differently. We are currently investigating the possibility of explaining the observed anomalies using the proton form factors of the analog resonances populated.

The authors wish to thank Dr. F. G. Perey and Dr. P. H. Stelson for help and hospitality offered during data acquisition at the Oak Ridge National Laboratory. We also acknowledge helpful discussions with Professor W. R. Coker, Professor C. F. Moore, and Professor T. Tamura.

*Work supported in part by U. S. Atomic Energy Commission.

¹R. L. McGrath, N. Cue, W. R. Hering, L. L. Lee, Jr., B. L. Liebler, and Z. Vager, Phys. Rev. Lett. **25**, 682 (1970); P. J. Cooney, N. Cue, R. L. McGrath, and H. Rudolph, Bull. Amer. Phys. Soc. **15**, 625 (1970).

²C. L. Hollas, J. Horton, P. J. Riley, S. A. A. Zaidi, C. M. Jones, and J. L. C. Ford, Bull. Amer. Phys. Soc. **14**, 1238 (1969).

³R. J. Couch, dissertation, Northwestern University, 1969 (unpublished), and ORNL Report No. ORNL-TM-2729, 1969 (unpublished).

⁴J. B. Moorhead and R. A. Moyer, Phys. Rev. **184**, 1205 (1969).

⁵S. A. Hjorth and B. L. Cohen, Phys. Rev. **135**, B920

(1964).

⁶B. L. Cohen and O. V. Chubinsky, Phys. Rev. **131**, 2184 (1963).⁷C. F. Moore, P. Richard, C. E. Watson, D. Robson, and J. D. Fox, Phys. Rev. **141**, 1166 (1966).⁸R. R. Jones, thesis, University of Texas, 1970 (unpublished); C. F. Moore, R. R. Jones, P. Dyer, N. Williams and G. C. Morrison, to be published.⁹J. Picard and G. Bassani, Nucl. Phys. **A131**, 636 (1969).

Coupled-Channel Born-Approximation Calculation of Two-Nucleon Transfer Reactions in Deformed Nuclei

T. Tamura

Center for Nuclear Studies, University of Texas, Austin, Texas 78712*

and

D. R. Bes, R. A. Broglia,† and S. Landowne‡

School of Physics,‡ University of Minnesota, Minneapolis, Minnesota 55455

(Received 12 October 1970)

Two-neutron transfer reactions in strongly deformed nuclei are discussed in the framework of the coupled-channel Born approximation. In particular, the reaction $^{176}\text{Yb}(p,t)^{174}\text{Yb}$ is analyzed.

The amplitude of the coupled-channel Born approximation (CCBA) for a transfer reaction $A(a,b)B$ with $a=b+x$, may schematically be written as¹

$$T = \langle \Psi_b^{(-)}(s_A+x, x_b, r_b) | V(x, x_b) | \Psi_a^{(+)}(x_A, x_a, r_a) \rangle, \quad (1)$$

where the wave functions $\Psi^{(\pm)}$ are solutions of appropriate coupled-channel equations² that describe the inelastic scattering on an essentially equal footing with the elastic scattering. Thus (1) is a natural extension of the distorted-wave Born-approximation (DWBA) amplitude in which the $\Psi^{(\pm)}$ describe only elastic scattering.

Equation (1) has been applied exactly only in very few cases so far.³ Ascuitto and Glendenning⁴ developed the so-called "source term" method which uses a different approach from the usual CCBA but is believed to yield an amplitude that agrees with (1). They performed calculations⁵ for (p,t) processes between moderately collective nuclei (Ni) and found that CCBA predicts, for example, twice as large a cross section to the collective 2^+ state as the normal DWBA calculation does. In the present article we apply (1) to a (p,t) process between two strongly deformed nuclei, and compare the results with those of corresponding DWBA calculations.⁶

In CCBA, the functions $\Psi^{(\pm)}$ in (1) may very explicitly be written as

$$\begin{aligned} \Psi_{m_a' M_{nA}'; m_a M_{nA}}^{(-)} = & \frac{4\pi}{k_a r_a} \sum_i i_a' (\hat{l}_a' / \hat{l}_a) \chi_{l_a' j_a' n_A'; l_a j_a n_A}^J(r_a) (l_a m_{l_a} s_a m_a | j_a m_{j_a}) (j_a m_{j_a} I_{nA} M_{nA} | JM) \\ & \times (l_a' m_{l_a'} s_a m_a' | j_a' m_{j_a'}) (j_a' m_{j_a'} I_{nA'} M_{nA'} | JM) Y_{l_a m_{l_a}}^*(\Omega_{\vec{k}_a}) \\ & \times Y_{l_a' m_{l_a'}}(\Omega_{\vec{k}_a}) \phi_{I_{nA} M_{nA}}(x_A) \varphi_{s_a m_a}(x_a), \end{aligned} \quad (2a)$$

$$\Psi_{m_b' M_{nB}'; m_b M_{nB}}^{(+)} = (-)^{I_{nB} - I_{nB}' + m_b' - m_b + M_{nB}' - M_{nB}} \Psi_{-m_b' - M_{nB}'; -m_b - M_{nB}}^{(-)}. \quad (2b)$$

Since we use a notation very similar to that used in Ref. 2 and by Satchler⁷, the meaning of (2) is clear. We just note that the function $\chi_{l_a' j_a' n_A'; l_a j_a n_A}^J(r_a)$ describes the radial part of the relative motion between A and a with angular momenta (l_a', j_a') , in the channel in which A lies in its n_A' th state, when the only incoming wave present is the one having angular momenta (l_a, j_a) in the channel in which A lies in its n_A th state. The superscript J is the total angular momentum of this set of coupled partial waves, while $\phi(x_A)$ and $\varphi(x_a)$ are internal wave functions of A and a , respectively.

Inserting (2) into (1) and performing algebra which extends that of Ref. 7, the amplitude (1) under